VOLUMETRIC SNAPPING: WATERTIGHT TRIANGULATION OF POINT CLOUDS

Tim Volodine[1], Michael S. Floater[2] and Dirk Roose[1]
[1] *KULeuven, Department of Computer Science, Celestijnenlaan 200A, 3001 Heverlee, Belgium*

[2] *CMA/IFI, University of Oslo, P.O.Box 1053 Blindern, 0316 Oslo, Norway*

Keywords: Meshing, surface reconstruction, volumetric grid, contouring, point clouds.

Abstract: We propose an algorithm which constructs an interpolating triangular mesh from a closed point cloud of arbitrary genus. The algorithm first constructs an intermediate structure called a Delaunay cover, which forms a barrier between the inside and the outside of the object. This structure is used to build a boolean voxel grid, with cells intersecting the cover colored black and all other cells colored white. The outer surface of the voxel grid is snapped to the point cloud by replacing each exterior surface vertex with the closest point in the point cloud. The snapped mesh is processed such that it is manifold and consists of triangles with good aspect ratio. We show that if a fine voxel grid is used, the snapping yields Delaunay-like triangulation of the original points. High grid resolutions are possible because of the Delaunay cover and a new contouring method, which extracts the outer surface of the grid with $O(n^2)$ worst case space complexity, where n is the number of voxels in one dimension.

1 INTRODUCTION

Nowadays 3D laser scanners are widely used to digitize real-world objects for visualisation, reverse engineering, inspection and animation. They produce huge amounts of point data, sampled from the surface of an object. While there are upcoming techniques for manipulating point data directly (Szeliski and Tonnesen, 1992; Pauly et al., 2006), the mesh representation still remains a widespread standard for manipulating and exchanging geometrical data. Therefore, the problem of approximating a point cloud with a polygonal mesh is an active topic of research.

Most scanners produce a very dense set of samples, not all of which are required in the final mesh. Therefore, to save time and space, an implicit volumetric representation of the point cloud is often used. Reconstruction algorithms based on the implicit approach typically involve an approximation of the signed distance function, which is supplied to an iso-surfacing method, such as Marching Cubes algorithm (Lorensen and Cline, 1987), to extract the mesh.

However, the construction of a signed distance function requires an oriented point cloud, i.e. a point cloud with consistently oriented normals. This kind of information is usually not available, significantly complicating the reconstruction process. Furthermore, in the presence of noise and overlapping scans, the signed distance function often results in topological artifacts as pointed out in (Hornung and Kobbelt, 2006; Wood et al., 2004). To overcome this problem, a volumetric method that does not rely on a signed distance function was proposed recently by Hornung and Kobbelt (Hornung and Kobbelt, 2006). They formulate the reconstruction problem as a minimal cut problem of a spatial graph defined on a voxel grid representation of the point cloud. The edges in the graph are weighted by confidence values, which can be interpreted as an unsigned pseudo-distance of a voxel to the closest point sample.

In this paper we propose a new volumetric method that is relatively simple to implement and gives good results in practice. Like the method of (Hornung and Kobbelt, 2006) we avoid computing a signed distance function. The main idea is to snap the triangulated exterior surface of the voxel grid to the point cloud. But in order to obtain a watertight voxelization at various resolutions we voxelize an intermediate structure, which is a union of triangle fans defining a barrier between the inside and the outside of the point cloud. Because the construction of this structure is based

Volodine T., S. Floater M. and Roose D. (2007).
VOLUMETRIC SNAPPING: WATERTIGHT TRIANGULATION OF POINT CLOUDS.
In *Proceedings of the Second International Conference on Computer Graphics Theory and Applications - GM/R*, pages 53-60
DOI: 10.5220/0002079800530060
Copyright © SciTePress

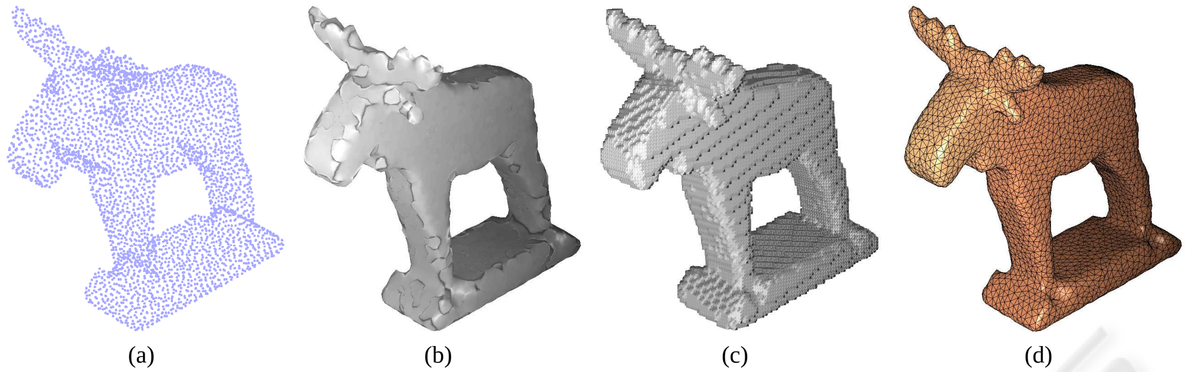

Figure 1: The 4 main steps of the algorithm: (a) the Moose point cloud with 3K points (b) Delaunay cover (c) voxel grid (d) mesh after snapping.

on *Delaunay neighborhoods* (Floater and Reimers, 2001), we call it a *Delaunay cover* of the point cloud.

The proposed algorithm guarantees a watertight reconstruction, it can deal with noisy data or overlapping scans, and can reconstruct meshes of a large number of points at various levels of detail. In addition our algorithm reconstructs convex sharp features without any additional information, like the Hermite data used in the Dual Contouring method (Ju et al., 2002). Contrary to the traditional contouring algorithms e.g. Marching Cubes and Dual Contouring, the reconstructed mesh is *interpolatory*, with all the vertices belonging to the original point cloud.

There are six conceptual steps in the proposed algorithm: construction of the Delaunay cover, voxelization, triangulation, snapping, clean-up and optimization. First, the Delaunay cover is constructed and voxelized into a regular voxel grid. Each voxel is colored either black (non-empty) or white (empty), depending on whether it intersects the Delaunay cover or not. Subsequently the exterior surface of the black voxels is triangulated, yielding a first watertight approximation of the point cloud. This approximating mesh is then *snapped* to the point cloud, with each voxel corner replaced by the nearest point in the point cloud. The snapping produces a geometric realisation of the voxel surface triangulation with the same watertight topology. Since the snapping is in general not injective, it yields degenerate and double triangles. However, all such triangles are removed in a simple clean-up step and this results in a valid manifold mesh. Finally, when a coarse grid is used for snapping, the obtained triangulation can be improved by an optimization step. In this step the vertices are diffused over the surface of the object in a manner similar to the shrink-wrapping process of (Kobbelt et al., 1999).

The task of triangulating the exterior voxel surface is accomplished by a 2D tracing algorithm, which processes the voxel grid slice by slice. The Delaunay cover and the space efficient contouring algorithm allow to use small voxels. We show that, with increasing grid resolution, the snapped triangulation converges to Delaunay-like triangulation of the points.

2 RELATED WORK

Depending on the topology of the geometry (sampling) of the point cloud, various methods for surface reconstruction have been proposed in the literature. We distinguish 4 main approaches: the implicit approach (Hoppe et al., 1992; Curless and Levoy, 1996; Carr et al., 2001; Ohtake et al., 2003), methods based on 3D Voronoi diagram (Amenta et al., 2001; Dey, 2006; Edelsbrunner and Mücke, 1994), advancing front algorithms (Bernardini et al., 1999; Scheidegger et al., 2005) and meshless parameterization (Floater and Reimers, 2001; Zwicker and Gotsman, 2004).

Related to the snapping idea is the approach of Kobbelt et al. (Kobbelt et al., 1999) for remeshing genus-0 polygonal surfaces into meshes with subdivision connectivity. The method simulates wrapping of a plastic membrane around an object by starting with a base mesh and iteratively applying projection, smoothing and subdivision operators to it. In (Jeong and Kim, 2002) Jeong et al. use the shrink-wrapping approach to create a mesh of a genus-0 point cloud by subdividing and shrink-wrapping its bounding box.

3 OVERVIEW

The algorithm consists of 6 steps,

1. Construct Delaunay Cover
2. Voxelize the Delaunay Cover
3. Triangulate the voxel grid surface
4. Snap the triangulated voxel surface to the point cloud
5. Clean-up the triangulation (to obtain a manifold triangulation)
6. (Optionally) optimize.

Note that the optimization step is only required when the voxel grid is relatively coarse. In the following sections we explain each of these steps in more detail.

4 DELAUNAY COVER

In order for the voxel surface to separate the inside and the outside of the shape it needs to be closed. If the voxelization is applied directly to the point cloud it may result in holes in places where the sampling density is larger than the grid size. To overcome this problem we use an intermediate structure, called the *Delaunay cover* of the point cloud. It consists of a collection of triangles, which define a barrier between the inside and the outside regions.

To explain the concept of a Delaunay Cover we need a couple of definitions. First we need the notion of the *local planar Delaunay triangulation* at p_i, which is the Delaunay triangulation of the projection of the k nearest neighbors of p_i on the tangent plane at p_i. The tangent plane is usually approximated by the least squares plane through the k nearest neighbors. The local planar Delaunay triangulation induces a *local triangulation* at p_i of the original k nearest neighbors in the point cloud P.

Definition 1 (Delaunay Fan) *A* Delaunay fan *$DFan(p_i)$ of p_i is the set of triangles in the local triangulation of p_i sharing p_i as their common vertex.*

Definition 2 (Delaunay Cover) Delaunay cover *$DC(P)$ of a point cloud P is the union of all the triangles in the Delaunay fans of each point in the point cloud, i.e. $DC(P) = \cup_{p_i \in P} DFan(p_i)$.*

In the planar case, when all points are in the plane and no four of them are cocircular, the Delaunay cover is simply the Delaunay triangulation of the points. In 3D the Delaunay cover approximates the point cloud, but is neither a consistent triangulation, nor does it have correctly oriented triangle normals, see figure 1(b).

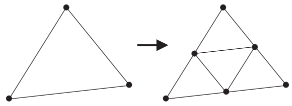

(a)

Figure 2: Refinement of the Delaunay cover : the triangle is subdivided if one of its sides is longer than the voxel side length. The new inserted vertices are the midpoints of the triangle edges.

5 VOXELIZATION OF THE DELAUNAY COVER

To voxelize the Delaunay cover into a regular voxel grid, we could use the triangle-voxel intersection test. In this approach a voxel is colored black if it is intersected by a triangle and it is white otherwise. It is possible to implement this kind of scan-conversion efficiently using an octree and the Separating Axes method for the intersection test, see (Ju, 2004). However in our algorithm we use a simpler technique to color the voxels without computing intersections and avoiding the construction of an octree.

5.1 Refinement of the Delaunay Cover

Let h be the voxel grid size (if the voxels are rectangular, let h be the minimal voxel edge length). In order to obtain a proper voxelization, it is sufficient to sample the Delaunay cover so that the distance between the sample points is smaller than h. The sampled points can then be used to create a voxelization in a straightforward way as explained later in 5.2.

To achieve the required sampling density we refine the triangles in the Delaunay cover using a 1-to-4 triangle split, as shown in figure 2. For each triangle four new triangles are created if one of the triangle sides is longer than h. The refinement is performed iteratively until all triangles have sides of length smaller than h. The refinement sequence can be written as $DC^0(P) \rightarrow DC^1(P) \rightarrow DC^2(P) \rightarrow \ldots \rightarrow DC^\kappa(P)$. With each $DC^i(P)$ there is an associated point cloud P^i.

5.2 Voxelization of the Refinement

The refinement of the Delaunay cover produces a set of refined points P^κ. To compute the voxel grid of this point cloud, its bounding box, represented by the corners $(x_{min}, y_{min}, z_{min})^\top$ and $(x_{\max}, y_{\max}, z_{\max})^\top$, is divided into cells of side length h. An example of such a voxelization is shown in figure 1(c). In our implementation we use a boolean voxel grid, represented

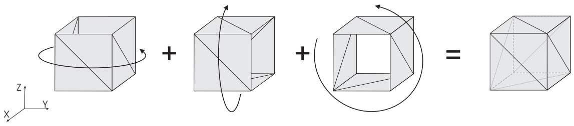

Figure 3: The three stripes parallel to the XY-plane, XZ-plane and YZ-plane are combined to obtain a triangulation of the voxel.

by a 3D matrix $V \in \mathbb{Z}_2^{n_x \times n_y \times n_z}$, where n_x, n_y and n_z is the number of voxels in the corresponding dimension. The matrix has a nonzero entry iff the corresponding voxel contains at least one point $p_i = (x_i, y_i, z_i)$ in P^κ. Starting with the zero matrix V, the voxelization is obtained by setting

$$V\left(\left\lfloor \frac{x_i - x_{min}}{h} \right\rfloor, \left\lfloor \frac{y_i - y_{min}}{h} \right\rfloor, \left\lfloor \frac{z_i - z_{min}}{h} \right\rfloor\right) = 1.$$

However, the memory consumption of this approach poses a problem, because the classical representation of a 3D matrix grows as a cube of the number of cells in each dimension. Fortunately, the matrix V will typically be very sparse, so the memory problem can be avoided by using a sparse representation of V. Our sparse representation stores only the nonzero entries in a hash table. This approach is both extremely fast and memory efficient.

6 TRIANGULATION OF THE VOXEL GRID SURFACE

We construct a consistent triangulation of the voxelgrid by processing it slice by slice in 3 directions (X, Y and Z). A slice is a 2D submatrix of V where one of the 3 dimensions is fixed, e.g. the first horizontal slice in the Z-direction is given by $B = V(\cdot, \cdot, 1)$. As shown in figure 3 the cube (one voxel) is completely and consistently covered by overlaying three triangle strips. The overlaid strips may cover some of the voxel faces two times. This is easily resolved by removing double triangles. For convex objects any two striping directions are actually sufficient to cover the whole surface. However for more complicated objects, e.g. the torus, we need 3 directions to be certain that the whole grid surface is covered.

6.1 The Contouring Algorithm

The contouring algorithm operates on a slice of V, which is a 2D submatrix $B \in \mathbb{Z}_2^{n_x \times n_y}$ (if the slice is in the Z-direction). It traces the contour counterclockwise around the nonzero (gray) entries in B, as shown in figure 5(a). Starting with the rightmost non-empty cell, we start moving upwards and always keep the gray cells to the left of the tracing direction.

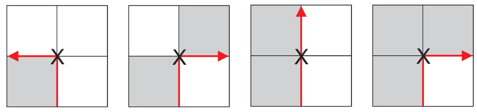

(a) (b) (c) (d)

Figure 4: The four cases for the tracing algorithm.

The tracing algorithm can be implemented by observing that there are only 4 cases to consider during tracing. They are depicted in figure 4. Imagine we are at position X in the figure, having just traced the vertical line below it. To decide where to go next we need to look at the content of the four neighboring cells. The four cases in the figure are the possible cases, all other configurations can be reduced to these 4 cases by rotation.

The traced 2D contour is used to create a triangulation of the outer surface of the slice. We create 2 parallel contours in 3D by lifting the traced 2D contour to 3D and offsetting it with the cell size in the third dimension. The outer surface of the slice is the quad strip of voxel faces contained between two contours. These voxel faces are triangulated by connecting the corresponding points (see figure 3).

If B contains multiple contours, they are extracted by applying the tracing algorithm multiple times. Each time a contour is extracted all the cells it encloses are filled with zeros and the tracing algorithm is repeated.

6.2 Contouring Cropped Grids

The contouring algorithm can be extended to handle holes lying on the boundaries of the bounding box. This extension allows the reconstructed mesh to be cropped by shrinking the bounding box. In order for the contouring algorithm to work with holes, the original matrix B is augmented with a boundary layer of non-empty entries. When applying the tracing algorithm in the presence of a hole, it produces a dual contour as shown in figure 5(b). The final contour is obtained by removing the traced segments between c_1 and c_2.

7 SNAPPING

Voronoi diagrams can be constructed by adaptively subdividing and sampling the space using an octree (or a quadtree in 2D), see e.g. (Lavender et al., 1992; Boada et al., 2002). This approach is especially useful for *approximating* the generalized Voronoi diagram,

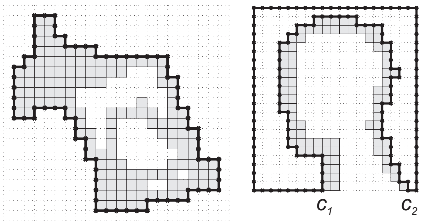

(a) (b)

Figure 5: (a) contour of a slice of the moose (b) dual contour of the slice of the mannequin head model with a hole.

where the sites are geometric primitives other than points.

Snapping the corners of a uniform triangulated grid to the closest points in the data set has a similar effect to the space sampling approach. In the following paragraph we show that snapping can be used to construct a Delaunay triangulation (the dual of the Voronoi diagram) of points in the plane. In 3D we sample the space in the vicinity of the Delaunay cover using voxel corners. If the voxels are smaller than the inter-point distances in the point cloud, we obtain an effect similar to the 2D situation, leading to a Delaunay-like triangulation of the surface points.

7.1 Delaunay Triangulation

Figure 6 illustrates the snapping algorithm in the plane. The red sample points are overlaid with triangulated grids (figures 6(a)-6(c)) with increasing resolutions. Figures 6(d)-6(f) show the resulting triangulations after snapping each grid point to the closest red point. Coarse grids produce a triangulation with overlapping triangles, or miss some of the original red points (figures 6(d) and 6(e)). Fine grids result in the Delaunay triangulation of the red points (figure 6(f)). The triangulation is actually the Delaunay triangulation plus various degenerate and repeated triangles, but these extra triangles are easy to remove.

To state a sufficient condition for obtaining the Delaunay triangulation we analyse the Voronoi diagram of the red points (e.g. figure 6(a)). In the Voronoi diagram we call two Voronoi cells neighbors if they share an edge. We define the distance between two cells as the shortest distance between any two points lying on the boundary of these cells. In this way the distance between neighboring cells is zero.

The sufficient condition for obtaining the Delaunay triangulation by snapping the grid is that the grid diagonals (longest triangle side) should be smaller than the distance between any two non-neighboring Voronoi cells. This condition also implies that degenerate cases, such as 4 or more points lying on a circle,

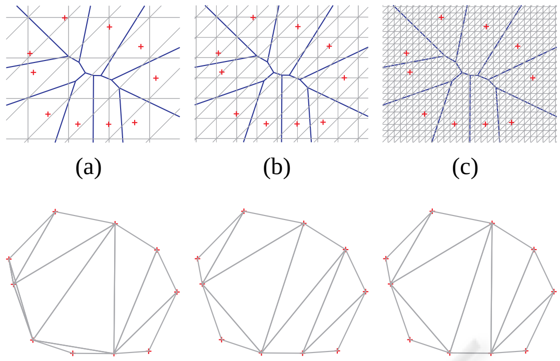

(a) (b) (c)

(d) (e) (f)

Figure 6: (a) cell size=0.6 (b) cell size=0.31 (c) cell size=0.1 (d) triangulation corresponding to (a), note the overlapping triangles; (e) triangulation corresponding to (b); (f) triangulation corresponding to (c), this is the Delaunay triangulation.

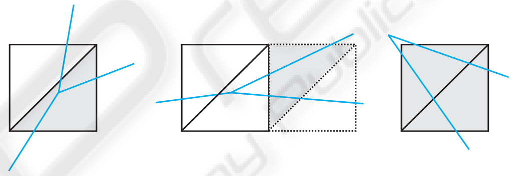

(a) (b) (c)

Figure 7: The three possible configurations in the snapping algorithm which yield non-degenerate triangles: (a) the gray triangle is snapped to a Delaunay triangle corresponding to the Voronoi vertex inside the grid cell (b) the gray triangle is snapped to the Delaunay triangle corresponding to the Voronoi vertex in the neighboring cell (c) both gray triangles are snapped to the same Delaunay triangle corresponding to the Voronoi vertex outside the grid cell.

cannot be Delaunay triangulated with the snapping algorithm, because in that case the distance between non-neighboring cells is zero.

To see why this condition is true we analyse the possible configurations of the grid cells w.r.t. the Voronoi diagram. Under above condition there are only three essential configurations which yield non-degenerate triangles after snapping. These cases are shown in figure 7. All three cases create only Delaunay triangles, sometimes multiple times (as in figure 7(c)).

8 CLEAN-UP

After snapping, the resulting triangulation is usually *not* a *topologically manifold* triangulation. By topologically manifold we mean that each point has a fan of triangles homeomorphic to a disc and each edge is

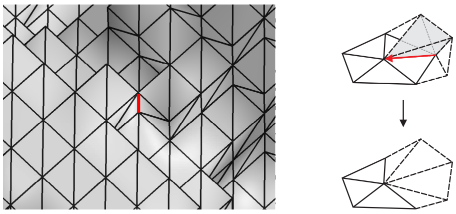

(a) (b)

Figure 8: (a) non-manifold edge on the outer surface of the voxel grid (b) collapse of a non-manifold edge.

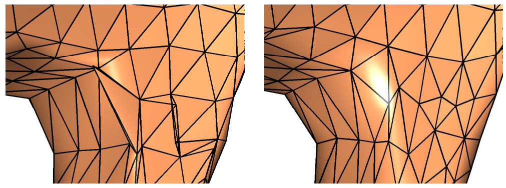

(a) (b)

Figure 9: Illustration of how the smooth-snap iteration resolves folded triangles; (a) folded triangles near the leg of the moose (b) mesh after one smooth-snap iteration.

shared exactly by two triangles. During the clean-up step we process the triangles such that the result is a manifold triangulation.

To obtain a manifold triangulation we remove the following items (in this order):

1. degenerate triangles (having at least two coinciding vertices)
2. multiple triangles (having the same vertices)
3. dangling triangles (which do not have three neighboring triangles)
4. non-manifold edges (edges shared by more than two triangles)

A degenerate triangle is created when two or three vertices of a voxel triangle are snapped to the same data point. Double triangles arise in cases as shown in figure 7(c). The removal of the first two items can occasionally result in dangling triangles, which are simply deleted from the triangulation. In some rare cases the triangulation of the exterior surface of the voxel grid can contain non-manifold edges, as shown on figure 8(a). To remove the non-manifold edges we collapse them, by snapping one end of the edge to the other, as shown in figure 8(b). Note that an edge collapse introduces degenerate and double triangles, which are cleaned up by executing the first three items once more.

9 OPTIMIZATION

The optimization step is only required when the voxel grid is coarse relative to the inter-point distance in the point cloud. The idea of the optimization step is to diffuse the vertices over the surface such that the position of each vertex is approximately at the center of its neighbors. The optimization is performed for two reasons. On the one hand, it improves the mesh quality and yields triangles with better aspect ratio. On the other hand, it unfolds locally folded triangles, which can occasionally appear after the snapping of coarse grids. Such triangles typically have a normal which is in the opposite direction to the normals of the neighboring triangles (figure 9(a)).

The optimization process is a number of smooth-snap iterations, consisting of two steps:

1. Smooth the manifold mesh and
2. Re-snap the smoothed mesh onto the point cloud.

In practice 1 or 2 iterations already give a significant improvement of the triangulation. We implemented the smoothing step using the simplest possible approach, i.e. Laplacian smoothing, where each vertex in the triangulation is replaced by the centroid of its neighbors. To obtain better diffusion we swap the edges in the 1-ring neighborhoods of vertices with valency 4, but only when no new valency 4 vertices are created by the edge swap.

10 RESULTS AND DISCUSSION

We applied the proposed meshing algorithm to different kinds of points clouds. The Moose point cloud (figure 1) is uniformly sampled. The Mannequin Head (figure 12) has adaptive sampling density, with more points in places of high curvature. In addition it illustrates the ability of the algorithm to handle point clouds with boundaries. Finally, the Cycladic Head model (figure 11) consists of a number of overlapping registered scans.

For both the Moose and the Mannequin Head data sets we used fine voxel grids *without* the optimization step (figures 12 and 1). Table 10 summarizes the algorithm statistics for the Moose model containing 10K points for different grid sizes. Note that there are no folded triangles for the finest grid resolution. We used a relatively coarse grid for the Cycladic Head model, followed by two smooth-snap optimization steps (figure 11).

The algorithm was implemented in C++ and executed on an Pentium 4 2.4Ghz machine with 512MB of RAM. The total time for the Moose 3K model was 4.8s, with the contouring step consuming 70% of the time. The Cycladic Head required a total of 76s,

grid size	DC-refinement	# grid vertices	nm edges[1]	degenerate	double	dangling	# folds[2]	final[3]
$14 \times 21 \times 22$	–	1010	0	52	0	0	34	984
$49 \times 78 \times 82$	43597	13759	7	9048	127	121	395	9116
$120 \times 192 \times 202$	208674	82948	1	144718	147	78	0	10502

[1] – number of non-manifold edges
[2] – number of folded fans
[3] – number of points in the final triangulation (after clean-up)

Figure 10: Statistics for the Moose 10K point cloud. Table shows the number of points, degenerate triangles, double triangles, dangling triangles, folded triangles and the number of points in the final triangulation for different grid sizes.

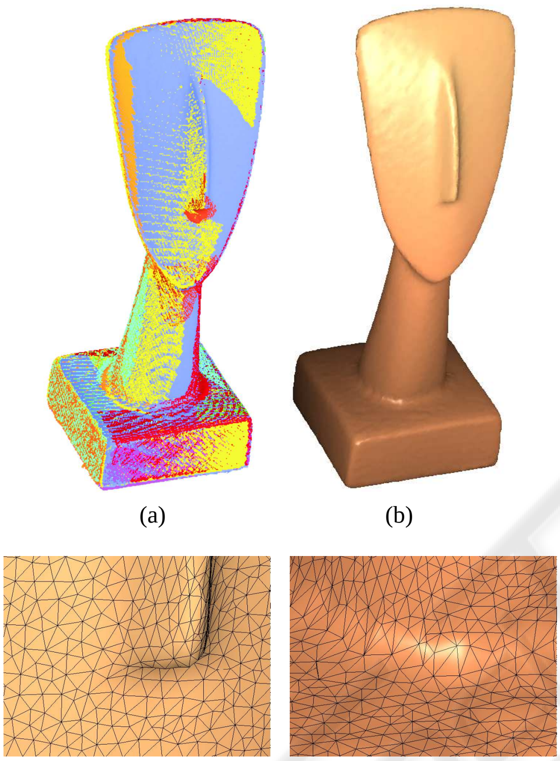

(a) (b) (c) (d)

Figure 11: (a) 9 aligned (registered) scans of the Cycladic Head point cloud, each scan has a different color (in total 190K points) (b) resulting mesh on a $61 \times 97 \times 102$ grid, 14K points and 28K triangles (c) close-up of the nose of the reconstructed mesh (d) close-up of the region near the socle of the model.

with 31% of the time spent on the construction of the Delaunay cover. The computation of the Delaunay cover requires a parameter k for the number of nearest neighbors. In our experience $k \in [15, 25]$ yields sufficient coverage for most point clouds. The snapping step is implemented using an octree structure, so that closest points can be located efficiently.

11 CONCLUSION

We found the method to work very well with real data obtained from a 3D laser scanner as well as filtered point clouds. It allows the construction of interpolating triangulations with various levels of detail by choosing the voxel size h. In order to obtain a closed voxelization we introduce the concept of a Delaunay cover. For filtered point clouds the Delaunay cover allows the use of small h, resulting in high quality triangulation of the points. For coarse grids the Delaunay cover may not be required, but in practice we always compute the Delaunay cover, otherwise it is difficult to determine the appropriate grid cell size. A limitation of the method is that it cannot be applied to point clouds with holes, unless the holes are aligned with the boundaries of the bounding box.

In our implementation we perform the extraction of the outer voxel surface by a 2D tracing algorithm, requiring $n_x + n_y + n_z$ slices of the voxel grid. An alternative is to use a 3D flooding algorithm, which would require $O((n_x + n_y + n_z)^3)$ storage, while our contouring algorithm has quadratic storage complexity.

ACKNOWLEDGEMENTS

We thank Martin Reimers for helpful discussions and for providing his software for inspection of non-manifoldness in triangulations. We thank the CMA, Oslo, for the use of their 3D scanner to generate the Moose and the Cycladic Head point clouds. This work was partly supported by the Project IUAP P5/22 of the Belgian Science Policy Office and the BeMatA program of the Norwegian Research Council.

REFERENCES

Amenta, N., Choi, S., and Kolluri, R. (2001). The power crust, unions of balls, and the medial axis transform. *Computational Geometry: Theory and Applications*, 19(2-3):127–153.

Bernardini, F., Mittleman, J., Rushmeier, H., Silva, C., and Taubin, G. (1999). The ball-pivoting algorithm for surface reconstruction. *IEEE Transactions on Visualization and Computer Graphics*, 5(4):349–359.

Boada, I., Coll, N., and Sellarés, J. (2002). Hierarchical planar voronoi diagram approximations. In *Proceedings of the 14th Canadian Conference on Computational Geometry*, pages 40–45.

Carr, J. C., Beatson, R. K., Cherrie, J., Mitchell, T. J., Fright, W. R., McCallum, B. C., and Evans, T. R. (2001). Reconstruction and representation of 3d objects with radial basis functions. In *ACM SIGGRAPH 2001*, pages 67–76.

Curless, B. and Levoy, M. (1996). A volumetric method for building complex models from range images. *Computer Graphics*, 30(Annual Conference Series):303–312.

Dey, T. K. (2006). *Curve and Surface Reconstruction: Algorithms with Mathematical Analysis*. Cambridge University Press.

Edelsbrunner, H. and Mücke, E. P. (1994). Three-dimensional alpha shapes. *ACM Transactions on Graphics*, 13(1):43–72.

Floater, M. and Reimers, M. (2001). Meshless parameterization and surface reconstruction. *Comp. Aided Geom. Design*, 18:77–92.

Hoppe, H., DeRose, T., Duchamp, T., McDonald, J., and Stuetzle, W. (1992). Surface reconstruction from unorganized points. In *ACM SIGGRAPH 1992*, pages 71–78.

Hornung, A. and Kobbelt, L. (2006). Robust reconstruction of watertight 3d models from non-uniformly sampled point clouds without normal information. In *Eurographics Symposium on Geometry Processing*, pages 41–50.

Jeong, W. and Kim, C. (2002). Direct reconstruction of displaced subdivision surface from unorganized points. In *Graphical Models*, volume 64(2), pages 78–93.

Ju, T. (2004). Robust repair of polygonal models. *ACM Trans. Graph.*, 23(3):888–895.

Ju, T., Losasso, F., Schaefer, S., and Warren, J. (2002). Dual contouring of hermite data. *ACM Trans. Graph.*, 21(3):339–346.

Kobbelt, L. P., Vorsatz, J., Labsik, U., and Seidel, H.-P. (1999). A shrink wrapping approach to remeshing polygonal surfaces. In *Computer Graphics Forum (Eurographics '99)*, volume 18(3), pages 119–130.

Lavender, D., Bowyer, A., Davenport, J., Wallis, A., and Woodwark, J. (1992). Voronoi diagrams of set-theoretic solid models. *IEEE Computer Graphics and Applications*, 12(5):69–77.

Lorensen, W. and Cline, H. (1987). Marching cubes: A high resolution 3d surface construction algorithm. *ACM Trans. Graph.*, 21(4):163–170.

Ohtake, Y., Belyaev, A., Alexa, M., Turk, G., and Seidel, H.-P. (2003). Multi-level partition of unity implicits. *ACM Trans. Graph.*, 22(3):463–470.

Pauly, M., Kobbelt, L. P., and Gross, M. (2006). Point-based multiscale surface representation. *ACM Trans. Graph.*, 25(2):177–193.

Scheidegger, C., Fleishman, S., and Silva, C. (2005). Triangulating point-set surfaces with bounded error. In *Proceedings of the third Eurographics Symposium on Geometry Processing*, pages 63–72.

Szeliski, R. and Tonnesen, D. (1992). Surface modeling with oriented particle systems. In *SIGGRAPH 1992, Computer Graphics Proceedings*, pages 185–194.

Wood, Z., Hoppe, H., Desbrun, M., and Schröder, P. (2004). Removing excess topology from isosurfaces. *ACM Trans. Graph.*, 23(2):190–208.

Zwicker, M. and Gotsman, C. (2004). Meshing point clouds using spherical parameterization. In *Proceedings of the Eurographics Symposium on Point-Based Graphics*.

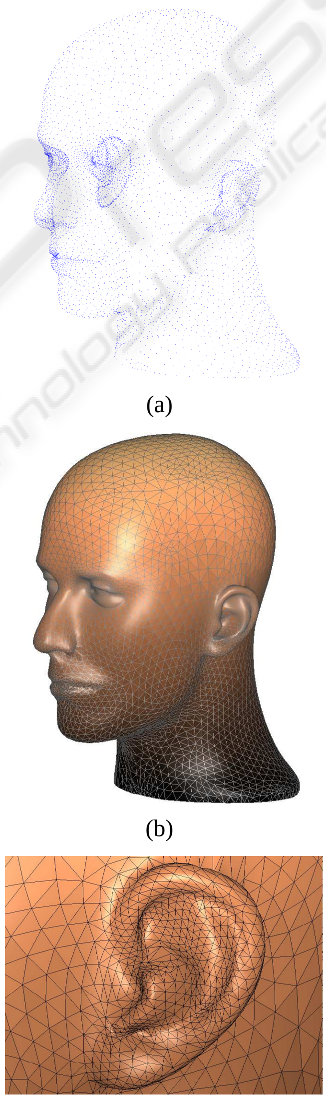

(a)

(b)

(c)

Figure 12: (a) point cloud of the Mannequin model (6K points) (b) reconstructed mesh on a $190 \times 253 \times 301$ grid (c) closeup of the ear.